ELSEVIER

Earth and Planetary Science Letters 204 (2002) 167–181

EPSL

www.elsevier.com/locate/epsl

^{147}Sm–^{143}Nd and ^{176}Lu–^{176}Hf in eucrites and the differentiation of the HED parent body

Janne Blichert-Toft *, Maud Boyet, Philippe Télouk, Francis Albarède

Ecole Normale Supérieure de Lyon, 69364 Lyon Cedex 7, France

Received 8 May 2002; received in revised form 10 September 2002; accepted 18 September 2002

Abstract

The ^{147}Sm–^{143}Nd and ^{176}Lu–^{176}Hf systematics of 21 whole-rock eucrites, including five cumulates, have been investigated by MC-ICP-MS. A statistically significant Sm–Nd isochron was obtained on 18 samples with an age of 4464 ± 75 Ma (MSWD = 1.26) and an intercept of 0.50680 ± 0.00010. This age clearly is controlled by the cumulate eucrites. The 21 basaltic and cumulate eucrites together do not form a statistically significant Lu–Hf isochron. Basaltic eucrites, however, form an errorchron with an age of 4604 ± 39 Ma (MSWD = 4.52), which becomes an acceptable isochron if the error on the Lu/Hf ratio is doubled with respect to the laboratory estimate. The initial $^{176}Hf/^{177}Hf$ is 0.27966 ± 0.00002. Three of the cumulate eucrites regressed together further yield a statistically significant age of 4470 ± 22 Ma, indistinguishable from their Sm–Nd age. We therefore conclude that cumulate eucrites are ~100 Myr younger than basaltic eucrites and basaltic eucrites are close in age to the Solar System. There is no evidence in the present data to support a decay constant of ^{176}Lu significantly different from 1.93 10^{-11} yr^{-1} [Sguigna, Can. J. Phys., 60 (1982) 361–364]. The broad range of variation and strong correlation of Lu/Hf and Sm/Nd ratios require that eucrites are partial melts and not residual magmas. The relative Lu/Hf and Sm/Nd fractionation is controlled by the plagioclase to mafic mineral ratio in the residue. The steep correlation between these two ratios is explained by the enhancement of plagioclase saturation in the low-gravity field of the eucrite parent body. Basaltic eucrites probably formed as large-degree melts of a chondritic source. The strong Lu/Hf and Sm/Hf fractionation observed in cumulates clearly reflects the presence of residual ilmenite during melting: our preferred interpretation is that cumulates were impregnated by small-degree melts of ilmenite-bearing gabbros. Since pressure on the eucrite parent body never reaches the garnet stability field, this observation questions the ubiquitous presence of residual garnet in the mantle sources of magmas formed on larger planets such as the Moon, Mars, and possibly Earth.

Keywords: Lu–Hf system; Sm/Nd; eucrites; ^{176}Lu decay constant; garnet group; ilmenite fractionation

1. Introduction

Howardites, eucrites, and diogenites (HED) are among the earliest magmatic rocks of the Solar System. Diogenites are pyroxenitic cumulates, eucrites are basaltic rocks and gabbroic cumulates, and howardites are mechanical mixtures between

* Corresponding author. Tel: +33-4-7272-8488; Fax: +33-4-7272-8677.
E-mail address: janne.blichert-toft@ens-lyon.fr (J. Blichert-Toft).

0012-821X/02/$ – see front matter © 2002 Elsevier Science B.V. All rights reserved.
PII: S0012-821X(02)00976-7

eucrites and diogenites. The unique oxygen isotope compositions of HED meteorites [1,2] and their consistent exposure ages [3,4] strongly support a common origin of the HEDs from a single planetary body. Currently, the HEDs are believed to have been chipped off from the asteroid Vesta [5,6] or from Vesta-like asteroids (vestoids) [7] by large impacts.

There is no consensus on the petrologic conditions under which eucrites formed. For some [8] they represent primary melts from the parent body mantle, whereas for others (e.g. [9]) they are residual melts from a magma ocean. Part of the discussion about the differentiation of the HED parent body is reminiscent of the confronting concepts on lunar differentiation (e.g. [10–13]). Numerous outstanding reviews of the vast literature on HED petrogenesis exist (e.g. [14,15]) and need not be repeated here.

Currently, CAIs and angrites, because of their old ages and relatively simple histories, constitute our best absolute references for planetary chronology. The age of eucrites, provided a single best age can be established, likewise would represent an excellent reference for the chronology of planetary formation. Most internal ^{147}Sm–^{143}Nd isochrons on basaltic eucrites, such as Juvinas [16], Stannern [17], Y75011 [18], Caldéra [19] and still others (see [20]), have yielded ages close to that of the beginning of the Solar System. The presence of excess nuclides left by the extinct radioactivities of ^{53}Mn ($T_{1/2}$ = 3.7 Ma), ^{60}Fe ($T_{1/2}$ = 1.5 Ma), and ^{26}Al ($T_{1/2}$ = 0.7 Ma) [21–24] further indicates that the formation of the HED parent body took place only a few Myr after the onset of Solar System condensation. Moreover, ^{53}Mn–^{53}Cr internal isochrons demonstrate that the emplacement of basaltic eucrites on the surface of the HED parent body occurred almost immediately thereafter. In contrast, cumulate eucrites such as Serra de Magé [25] and Moama [26] tend to give slightly younger ages.

Although originally introduced more than 20 years ago by P.J. Patchett, M. Tatsumoto and coworkers, it was not until the recent advent of multiple-collector inductively coupled plasma mass spectrometry (MC-ICP-MS) that the ^{176}Lu–^{176}Hf long-lived isotope system ($T_{1/2} \sim 35$ Ga) finally became a routine-use chronometer. Although a true feat at the time, the early ^{176}Lu–^{176}Hf work on eucrites by Patchett and Tatsumoto [27] and Tatsumoto et al. [28] suffered from the poor sensitivity of thermal-ionization mass spectrometry (TIMS) for Hf, resulting in inadequate precision on $^{176}Hf/^{177}Hf$ ratios.

The Lu–Hf system is not just yet another chronometer, but a chronometer for which both the parent and daughter nuclides are both refractory and lithophile as well as incompatible. Only one other known chronometer, that of the ^{147}Sm–^{143}Nd pair, has these same critical properties. The Lu–Hf and Sm–Nd couples lack the volatile character shown by ^{87}Rb and Pb (and potentially Re) isotopes and the siderophile character shown by Os (and potentially Pb) isotopes. Despite the similarities between the Lu–Hf and Sm–Nd systems, they differ by their fractionation behavior during planetary formation. Whereas Hf can be incorporated into ilmenite [29,30], a mineral diagnostic of extreme magmatic fractionation, Lu, Sm and Nd are far more incompatible upon differentiation of a planetary object such as the HED parent body in which low gravity does not allow for garnet stability. Since much emphasis has been placed on Lu/Hf fractionation by garnet in the major magmatic processes involved in differentiating the large terrestrial planets [31–34], eucrites therefore represent a potentially interesting test case.

The present work reports a new whole-rock ^{176}Lu–^{176}Hf isochron on 21 eucrites, including five cumulate eucrites, some of which have not been previously analyzed. Since the decay constant λ_{176Lu} of ^{176}Lu, first determined by Patchett and Tatsumoto [27] and Tatsumoto et al. [28], is still somewhat uncertain (see [35] for a review and [36] for the most recent determination of this constant), an important by-product of this isochron would be an independent value of λ_{176Lu}. In order to further constrain the age of eucrites and compare their Hf and Nd isotopic properties, a whole-rock ^{147}Sm–^{143}Nd isochron was also determined. The combined Sm–Nd and Lu–Hf isotope work was carried out on the same eucrite aliquots, an imperative approach necessary to minimize ambiguities arising from sample heterogeneity given

Table 1
Hf isotope compositions of basalts as measured by both Glass Expansion and Aridus nebulizers

Sample	Region	$^{176}Hf/^{177}Hf$ $\pm 2\sigma/\sqrt{n}$	ε_{Hf}	$^{176}Hf/^{177}Hf$ $\pm 2\sigma/\sqrt{n}$	ε_{Hf}
Nebulizer		Glass Expansion		Aridus	
J1	Pacific Ocean	0.283061 ± 7	10.2	0.283058 ± 3	10.1
J6	Pacific Ocean	0.282903 ± 7	4.6	0.282921 ± 4	5.3
				0.282921 ± 4	5.3
J10	Pacific Ocean	0.283007 ± 6	8.3	0.283009 ± 7	8.3
				0.283008 ± 6	8.4
U160	Gulf of Aden	0.283144 ± 5	13.2	0.283132 ± 3	12.7
B-2	Hawaii	0.282949 ± 8	6.3	0.282951 ± 3	6.3
B-3	Hawaii	0.282978 ± 8	7.3	0.282992 ± 4	7.8
B-11	Hawaii	0.282935 ± 8	5.8	0.282934 ± 5	5.7
B-16	Hawaii	0.282937 ± 6	5.8	0.282951 ± 6	6.3
UW12	Columbia River	0.282859 ± 10	3.1	0.282869 ± 7	3.4
UW13	Columbia River	0.282870 ± 7	3.5	0.282873 ± 5	3.6

Hf isotopic compositions measured by MC-ICP-MS (VG Plasma 54). Uncertainties reported on Hf measured isotope ratios are in-run $2\sigma/\sqrt{n}$ analytical errors in last decimal place, where n is the number of measured isotopic ratios. $^{176}Hf/^{177}Hf$ normalized for mass fractionation to $^{179}Hf/^{177}Hf = 0.7325$. $^{176}Hf/^{177}Hf$ of JMC-475 Hf standard = 0.282160 ± 0.000010 (2σ) (i.e., external reproducibility = 35 ppm). Hf standard run alternately with samples. ε_{Hf} values calculated using $^{176}Hf/^{177}Hf_{CHUR(0)} = 0.282772$.

that many eucrites are coarse-grained and/or heavily shocked and only small samples generally can be obtained for analysis. However, despite acquiring the Lu–Hf and Sm–Nd data on the same powder aliquots allowing direct comparison of the behavior of these two systems in eucrites, the small sample sizes preclude any guaranteeing that true 'whole-rock' data are obtained and some resulting scatter is still likely.

2. Analytical techniques

The eucrites analyzed in this study were received from museum meteorite curators in the form of small chips free of fusion crust and varnished surfaces. The chips were crushed into fine powders under clean lab conditions using a boron–carbide mortar and pestle reserved exclusively for meteorite work. Depending on sample availability and Hf contents of individual eucrites, between 100 and 500 mg whole-rock samples were digested.

Samples were dissolved in steel-jacketed Teflon bombs. Mixed ^{176}Lu–^{180}Hf and ^{149}Sm–^{150}Nd spikes were added to the sample powders at the outset of the dissolution procedure. Upon complete sample-spike homogenization, Cr, which is abundant in most eucrites, was reduced and a Hf-bearing fraction subsequently separated from a rare earth element (REE) fraction on a cation-exchange column. The REE cut was loaded onto an HDEHP column and split into Nd, Sm, and Yb–Lu fractions. Hf was further purified, first through an anion-exchange column serving to remove remaining matrix elements, then through a cation-exchange column separating Ti and some Zr from the Hf. Only double-distilled reagents and new resins were used throughout the dissolution and elution procedures. Total procedural Lu, Hf, Sm, and Nd blanks were <20, <25, <20, and <200 pg, respectively, or at least a factor 1000 smaller than the processed amount of element for each eucrite. No duplicate analyses were possible due to insufficient sample material. The chemical separation techniques used for all four elements are described in detail in [37,38].

Isotopic analysis of Hf, Lu, Nd, and Sm was carried out by MC-ICP-MS on the VG Plasma 54 instrument in Lyon using an Aridus desolvating nebulizer for Hf and the standard Glass Expansion nebulizer for Nd, Sm and Lu. Hf isotopic analysis was done following the technique described in [37], while Sm and Nd isotopic analyses were done according to a modified procedure of [39]. The method employed for Lu isotope analy-

sis is described below. Table 1 shows Hf isotopic compositions for 10 terrestrial basalts as measured using both the Glass Expansion and Aridus nebulizers. All analyses are identical within the external reproducibility of 35 ppm (see below) for the two types of nebulizer, demonstrating the absence of isobaric interferences on the isotopes of Hf due to the use of nitrogen as the carrier gas in the Aridus nebulizer. Table 1 further shows the excellent reproducibility between individual Aridus runs owing to increased ion beam stability when using this nebulizer.

In order to monitor machine performance, the JMC-475 Hf and La Jolla Nd standards were run systematically before and after each sample and gave, throughout this study, 0.282160 ± 0.000010 for $^{176}Hf/^{177}Hf$ and 0.511858 ± 0.000018 for $^{143}Nd/^{144}Nd$ (two standard deviations), corresponding to an external reproducibility of 35 ppm for both elements.

So far, one of the limitations of the Lu–Hf dating technique, including the use of TIMS, has been the lack of an efficient and reproducible way of calculating the mass bias for Lu, which has only two isotopes. The common assumption usually made, notably for MC-ICP-MS measurements, is identical mass bias for Yb and Lu. Using this conjecture and analyzing these two elements simultaneously, Lu concentration determinations typically have errors of about 1%. In the context of the present work, a major improvement in the precision of measuring Lu concentrations was achieved by applying the external normalization technique described in [40]. First, standard solutions of pure Yb are run to establish the Yb mass discrimination line in a ln(176/171) vs. ln(174/171) plot. Second, mixed standard solutions of Yb and Lu analyzed systematically between samples make it possible to evaluate precisely the mass bias for $^{176}Lu/^{175}Lu$. Third, the interpolated values of the mass bias obtained in this way are applied to the spiked samples. Contrary to previous techniques, this method does not depend on knowledge of the true isotopic composition of Yb, which is currently poorly constrained, and results in an error on Lu concentration measurements better than 5‰.

Our ^{180}Hf and ^{150}Nd spikes are enriched to more than 98%. Adequate spike/sample ratios require a correction due to the presence of the spike of less than 0.2 epsilon units on $^{176}Hf/^{177}Hf$ and less than 1 epsilon unit on $^{143}Nd/^{144}Nd$. In contrast to this 'underspiking' criterium applied to Hf and Nd isotopic measurements, the 'optimum' spiking criterium [41] was applied to Lu and Sm concentration measurements. The ^{176}Lu–^{180}Hf and ^{149}Sm–^{150}Nd spikes were calibrated on the Plasma 54 using calibration curves and normal solutions prepared gravimetrically from pure Ames metals. The Sm–Nd and Lu–Hf isotope data for the 21 eucrites analyzed in this study are listed in Table 2 and shown in isochron diagrams in Figs. 1 and 2, respectively. The reproducibilities of $^{147}Sm/^{144}Nd$ and $^{176}Lu/^{177}Hf$ are conservatively estimated to be 0.5%. The statistical treatment of the data is explained in Appendix A.

3. Results

A striking feature of the present results is the large contrast in fractionation behavior between the Sm–Nd and Lu–Hf systems (Table 2 and Figs. 1 and 2). The five cumulates Moama, Moore County, Nagaria, Serra de Magé, and Talampaya stand out with higher Sm/Nd ratios than the basaltic eucrites. The $^{147}Sm/^{144}Nd$ ratios of the 16 basaltic eucrites fall in a remarkably narrow range (0.1906–0.2028) and their mean value (0.1966 ± 0.0017; $2\sigma_{mean}$) is identical to the mean chondritic value of [42]. The Lu/Hf ratios vary to a much larger extent. Again, the five cumulate eucrites have much higher ratios, by up to a factor of three, than the basaltic eucrites, but even the range in Lu/Hf ratios among the basaltic eucrites themselves varies by $\sim$50%. With the exception of Caldéra, basaltic eucrites have Lu/Hf ratios lower than chondritic, whereas the Lu/Hf ratios of cumulate eucrites are consistently higher. The mean $^{176}Lu/^{177}Hf$ ratio of the basaltic eucrites is 0.0295 ± 0.0014 ($2\sigma_{mean}$), i.e., significantly lower than the mean value of 0.0332 ± 0.0002 reported for chondrites [32].

The 21 eucrites together do not define an acceptable ^{147}Sm–^{144}Nd isochron, as Moama, Pa-

Table 2
Lu–Hf and Sm–Nd whole-rock isotope and concentration data for basaltic and cumulate eucrites

Sample	Split	Source[a]	[Lu][b] (ppm)	[Hf][b] (ppm)	$^{176}Lu/^{177}Hf$[b]	$^{176}Hf/^{177}Hf$[c] $\pm 2\sigma/\sqrt{n}$	[Sm][d] (ppm)	[Nd][d] (ppm)	$^{147}Sm/^{144}Nd$[d]	$^{143}Nd/^{144}Nd$[e] $\pm 2\sigma/\sqrt{n}$
Béréba	n° 1297	(1)	0.2611	1.281	0.02893	0.282367 ± 7	1.753	5.429	0.1952	0.512557 ± 11
Bouvante	n° 3223	(1)	0.4337	2.530	0.02433	0.281908 ± 3	3.402	10.79	0.1906	0.512442 ± 7
Cachari	1998.71	(2)	0.2546	1.147	0.03151	0.282587 ± 6	1.672	5.155	0.1961	0.512615 ± 11
Caldéra	n° 3393	(1)	0.2446	0.9783	0.03549	0.282947 ± 4	1.722	5.254	0.1982	0.512745 ± 12
Camel Donga	n° 3335	(1)	0.3149	1.601	0.02791	0.282287 ± 4	2.116	6.529	0.1959	0.512608 ± 13
Ibitira	1998.70	(2)	0.2718	1.197	0.03222	0.282677 ± 7	1.650	4.920	0.2028	0.512805 ± 15
Jonzac	n° 1457	(1)	0.2628	1.264	0.02949	0.282404 ± 4	1.666	5.098	0.1976	0.512647 ± 13
Juvinas	n° 40	(1)	0.2447	1.137	0.03053	0.282471 ± 5	1.576	4.843	0.1968	0.512633 ± 9
Lakangaon	BM 1915, 142	(3)	0.3468	1.720	0.02862	0.282319 ± 4	2.380	7.361	0.1955	0.512577 ± 16
Millbillillie	n° 3404	(1)	0.2622	1.259	0.02955	0.282398 ± 3	1.727	5.316	0.1963	0.512589 ± 13
Moama[f]	E12415	(4)	0.05882	0.07559	0.1104	0.289702 ± 14	0.1668	0.3917	0.2575	0.513817 ± 9
Moore County[f]	USNM 6649	(5)	0.1552	0.4829	0.04561	0.283862 ± 5	0.7846	2.251	0.2107	0.513043 ± 7
Nagaria[f]	BM 51368	(3)	0.07373	0.1453	0.07203	0.286140 ± 14	0.2504	0.6676	0.2268	0.513521 ± 8
Padvarninkai	BM 1931, 108	(3)	0.2567	1.129	0.03228	0.282633 ± 5	1.568	4.886	0.1940	0.512585 ± 6
Palo Blanco Creek	BM 1991, M.6	(3)	0.2508	1.360	0.02617	0.282135 ± 5	1.758	5.532	0.1921	0.512528 ± 12
Pasamonte	BM 1959, 756	(3)	0.2658	1.278	0.02951	0.282393 ± 4	1.745	5.249	0.2009	0.512590 ± 9
Peramiho		(6)	0.2442	1.049	0.03304	0.282752 ± 6	1.468	4.442	0.1998	0.512707 ± 7
Serra de Magé[f]	n° 1606	(1)	0.05473	0.1422	0.05462	0.284661 ± 11	0.2324	0.6744	0.2083	0.512954 ± 15
Sioux County	n° 2325	(1)	0.2580	1.271	0.02880	0.282333 ± 3	1.671	5.085	0.1986	0.512693 ± 10
Stannern	gl. nr. 19	(2)	0.4147	2.330	0.02530	0.282016 ± 4	3.189	10.09	0.1910	0.512467 ± 11
Talampaya[f]	BM 1999, M.67	(3)	0.03093	0.06692	0.06561	0.285775 ± 60	0.1021	0.2976	0.2074	0.512976 ± 16

[a] (1) Muséum National d'Histoire Naturelle, Paris; (2) Geologisk Museum, Copenhagen; (3) The Natural History Museum, London; (4) Museum Victoria, Melbourne; (5) Smithsonian Institution, National Museum of Natural History, Washington DC; (6) Naturhistorisches Museum, Vienna.

[b] Hf and Lu isotopic compositions and concentrations measured by MC-ICP-MS (VG Plasma 54). [Hf], [Lu], and $^{176}Lu/^{177}Hf < 0.5\%$ (2σ errors). Hf and Lu concentrations determined by isotope dilution.

[c] Uncertainties reported on Hf measured isotope ratios are $2\sigma/\sqrt{n}$ analytical errors in last decimal place, where n is the number of measured isotopic ratios. $^{176}Hf/^{177}Hf$ normalized for mass fractionation to $^{179}Hf/^{177}Hf = 0.7325$. $^{176}Hf/^{177}Hf$ of JMC-475 Hf standard = 0.282160 ± 0.000010 (2σ) (i.e., external reproducibility = 35 ppm). Hf standard run alternately with samples.

[d] Nd and Sm isotopic compositions and concentrations measured by MC-ICP-MS (VG Plasma 54). [Nd], [Sm], and $^{147}Sm/^{144}Nd < 0.5\%$ (2σ errors). Nd and Sm concentrations determined by isotope dilution.

[e] Uncertainties reported on Nd measured isotope ratios are $2\sigma/\sqrt{n}$ analytical errors in last decimal place, where n is the number of measured isotopic ratios. $^{143}Nd/^{144}Nd$ normalized for mass fractionation to $^{146}Nd/^{144}Nd = 0.7219$. $^{143}Nd/^{144}Nd$ of La Jolla Nd standard = 0.511858 ± 18 (2σ) (i.e., external reproducibility = 35 ppm). Nd standard run alternately with samples.

[f] Cumulate eucrites.

samonte and Caldéra visibly fall off the main trend (Fig. 1). The remaining 18 samples, by contrast, define a statistically significant isochron (MSWD = 1.26, with 25% of the misfit due to Padvarninkai, a eucrite containing shock melt [43]) with a slope of 0.02962 ± 0.00050, which corresponds to an age of 4464 ± 75 Ma and an intercept of 0.50680 ± 0.00010. The relatively large errors reflect the small spread in parent/daughter ratios. Although the present intercept is within error of earlier estimates, e.g. 0.50684 for Juvinas [16], the age of the whole-rock isochron is younger than literature data, which typically fall around 4.54 Ga. Nevertheless, literature data, in particular the eucrites analyzed by [20], plot well within errors of the present samples. Regressing the basaltic eucrites by themselves and leaving out Caldéra and Pasamonte still produces a statistically significant isochron (MSWD = 1.29), but now with a much larger error on the age (4303 ± 175 Ma) due to the small spread in parent/daughter ratios among the basaltic eucrites. Of relevance

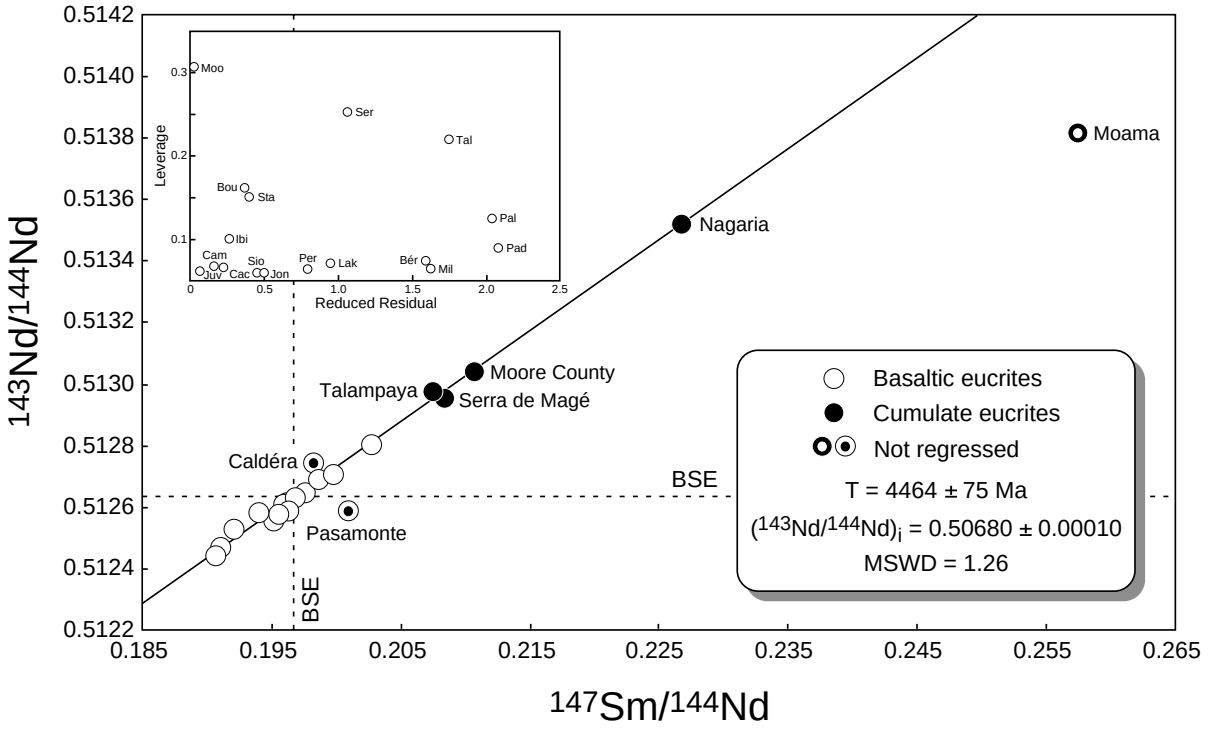

Fig. 1. Sm–Nd isochron diagram for basaltic and cumulate eucrites. Both *x*- and *y*-axis error bars are smaller than the symbols. Note that cumulate eucrites have consistently higher Sm/Nd ratios than basaltic eucrites. Note also the small variation in parent/daughter ratios among especially the basaltic eucrites for the Sm–Nd system compared with the Lu–Hf system (Fig. 2). The outliers, Caldéra, Pasamonte, and Moama, were not included in the regression calculation. The Sm–Nd reference for BSE is from [42] and plots within errors on the eucrite isochron. Inset: leverage vs. reduced residual diagram once the three outliers *and* Nagaria have been left out. The high leverages (see Discussion and Appendix A) of the cumulate eucrites Moore County, Serra de Magé, and Talampaya show that these samples together with Nagaria control the age of the Sm–Nd isochron.

to planetary evolution, the Sm–Nd bulk silicate earth (BSE) values of [42] plot within 0.2 epsilon units of the composite eucrite isochron (Fig. 1).

The 21 eucrite samples together do not form a statistically significant ^{176}Lu–^{176}Hf isochron either (Fig. 2) (MSWD = 6.87), but Nagaria and Palo Blanco Creek account for more than 25% of the misfit. However, even when these two samples are discarded from the regression, the isochron remains unacceptable (MSWD = 4.69). When basaltic eucrites are regressed separately, still with Palo Blanco Creek excluded, the MSWD stays high (4.52). The slope of 0.09294 ± 0.00080 corresponds to an age of 4604 ± 39 Ma (using $\lambda_{176Lu} = 1.93\ 10^{-11}\ yr^{-1}$) and an initial $^{176}Hf/^{177}Hf$ of 0.279660 ± 0.000024, which is lower by 2 epsilon units but still in marginal agreement within error bars with the initial $^{176}Hf/^{177}Hf$ back-extrapolated from the present-day measured values of chondrites [32]. We further note that an identical intercept of 0.27963 ± 0.00004 recently was established from a chondrite isochron (M. Bizzarro, unpublished data). In all cases, the Lu–Hf isochrons become statistically significant (i.e., MSWD ≤ 1.7) if an error of 1% (instead of the estimated 0.5%) for the Lu/Hf ratio is applied to the regression parameters. By contrast, three of the cumulate eucrites regressed together (Moama, Moore County, and Serra de Magé) define a perfect alignment with an age of 4470 ± 22 Ma (using $\lambda_{176Lu} = 1.93\ 10^{-11}\ yr^{-1}$). The Lu–Hf BSE values of [32] fall about 1 epsilon unit above the eucrite isochron (Fig. 2).

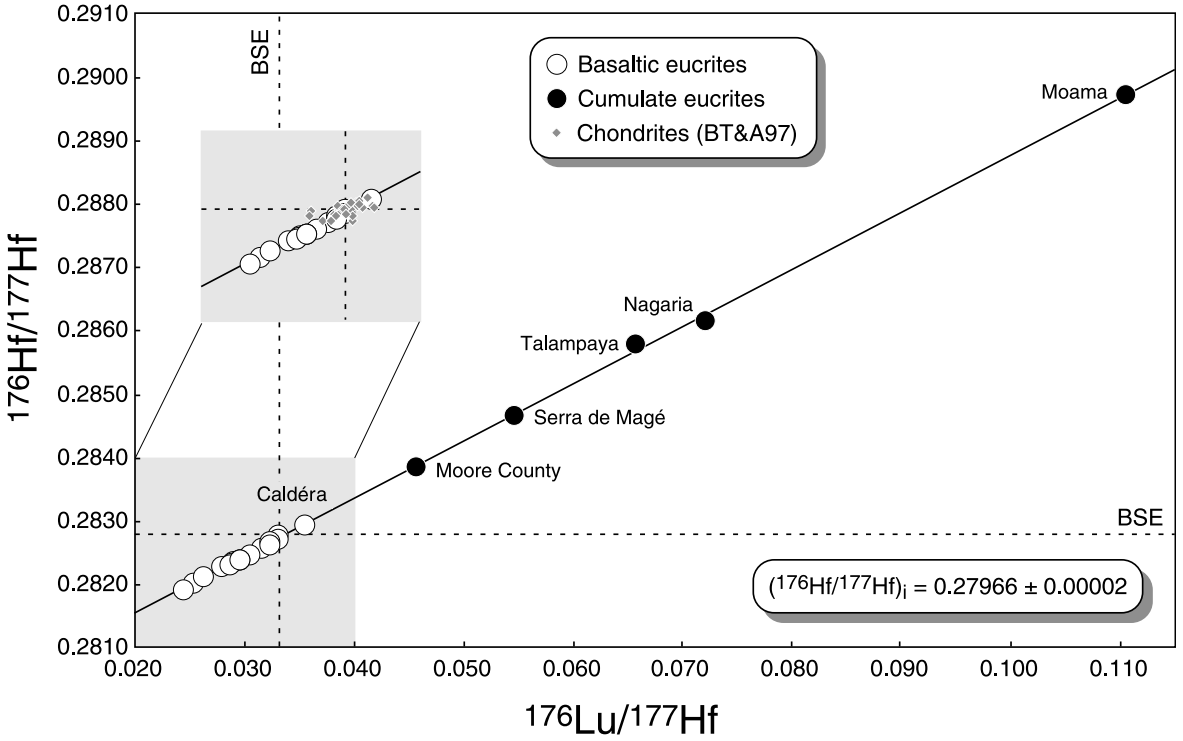

Fig. 2. Lu–Hf isochron diagram for basaltic and cumulate eucrites. Both *x*- and *y*-axis error bars are smaller than the symbols. Note the relatively large spread in parent/daughter ratios among even the basaltic eucrites for the Lu–Hf system compared with the Sm–Nd system (Fig. 1). Note also that the Lu–Hf reference for BSE as measured on 25 chondrites of different classes by [32] (BT & A97; shown in shaded inset) plots within errors on the eucrite isochron and divides cumulate (Lu/Hf ratios higher-than-chondritic) from basaltic (Lu/Hf ratios lower-than-chondritic) eucrites. Caldéra is a highly recrystallized impact melt [19], which could explain why this basaltic eucrite has slightly higher-than-chondritic Lu/Hf compared to the other basaltic eucrites: it may have assimilated some local (cumulative?) and/or impactor material.

4. Discussion

There is so far no consensus on the age of eucrites. In favor of a very early mantle source differentiation, Lugmair and Shukolyukov [21] obtained a significant ^{53}Mn–^{53}Cr whole-rock isochron including both basaltic and cumulate eucrites. Chromium isotopic disequilibrium among the minerals of many basaltic eucrites further suggests very early eruption of basalts at the surface of the eucrite parent body. Likewise, Ni isotopic disequilibrium between different mineral phases from the Juvinas basaltic eucrite indicates the presence of live ^{60}Fe when these minerals crystallized [23]. By contrast, there is no Cr isotope disequilibrium in the Moore County cumulate eucrite and evidence from Serra de Magé is ambiguous [21].

Evidence in favor of young eucrite crystallization ages is abundant. The most precise ages indicated by ^{147}Sm–^{143}Nd and Pb-Pb mineral isochrons on eucrites vary from ages in excess of 4.54 Ga to ages as young as 4.41 Ga (see [20] for a review). It has been known for some years now that cumulate and basaltic eucrites are not related by simple fractionation processes [8]. There is a distinct possibility [20] that cumulate eucrites as a group are significantly younger than basaltic eucrites. The ambiguity of whole-rock isochrons is that they do not necessarily date the simultaneous eruption of the constitutive samples but rather reflect the timing of mantle source dif-

ferentiation (mantle isochrons). The ambiguity of mineral (internal) isochrons is that they may date closure as well as resetting of chronometric systems, for example by impacts. Persisting ^{53}Cr and ^{60}Fe disequilibrium among minerals and ^{39}Ar–^{40}Ar plateau ages commonly in the 3.5–4.0 Ga range [44] support the second option.

4.1. Sm–Nd ages of eucrites

Small relative Sm/Nd fractionation among basaltic eucrites precludes a useful age to be derived from a ^{147}Sm–^{144}Nd isochron restricted to these samples only. We therefore have no better option than to try to derive adequate age information from the composite cumulate–basaltic eucrite isochron (Fig. 1), which gives an age of 4464 ± 75 Ma. The three eucrites that fall off the ^{147}Sm–^{144}Nd isochron (Caldéra, Moama, and Pasamonte) correspond noticeably to three of four eucrites that have been shown recently to display significantly higher $\Delta^{17}O$ than other eucrites [2]. The fourth eucrite with an anomalous oxygen isotopic composition, Ibitira, does not stand out for Sm–Nd. The oxygen isotope results suggest that these anomalous eucrites may have incorporated substantial amounts of the impactor. This remarkable coincidence between aberrant oxygen and Sm–Nd isotopic compositions combined with the fact that Caldéra is a highly recrystallized impact melt [19], while Pasamonte is heavily brecciated, vindicates the present ^{147}Sm–^{144}Nd isochron age.

The age of the Sm–Nd isochron is strongly controlled by the cumulate eucrites and this can be understood in terms of the relatively simple statistical concepts of leverage (see also Appendix A), a measure of the extent to which a given point accounts for the value of the slope or intercept. A point with very small leverage has no influence on these parameters. In the most extreme case, that of a two-point isochron, each of the two points has a leverage of one. For a straight line, leverage numbers sum to two. Because of its high Sm/Nd ratio, the Nagaria cumulate eucrite has a fairly large leverage of 0.58, compared to about 0.05 for each of the basaltic eucrites (Fig. 1, inset). This designates Nagaria as controlling the age of the isochron and suggests calculating the same isochron without it. As expected, the error on the age increases by 60%, but the age, now controlled by Moore County, Serra de Magé, and Talampaya (leverages of 0.22–0.30; Fig. 1, inset), remains unchanged (4461 ± 114 Ma). We therefore conclude that, in agreement with previous findings (e.g. [20]), the composite whole-rock isochron reveals the age of the cumulate eucrites, or at least the age of the last differentiation of their mantle source, which in turn post-dates the formation of the Solar System by about 100–150 Myr.

4.2. Lu–Hf ages of eucrites and the decay constant of ^{176}Lu

We cannot enter into the discussion about the ^{176}Lu–^{176}Hf age(s) of eucrites without first reviewing the increasingly controversial issue of ^{176}Lu decay. The rate of decay of ^{176}Lu by β^- emission is currently not well-constrained (see [35] for a review). Early laboratory measurements were plagued with the difficulty of counting low-energy electrons and although most modern counting experiments detect gamma emissions rather than the electrons themselves, physical counting techniques are still left with a number of hampering analytical problems. The early physical determination of [45] resulting in $\lambda_{176Lu} = 1.93\ 10^{-11}\ yr^{-1}$ pervaded the literature for years but gradually became superseded by the more precise physical determinations of [46,47], which by gamma spectrometry found values indicating a slower decay rate for ^{176}Lu. A significant first empirical estimate applying a geological comparison was that of [27,28], who used an age of 4.55 Ga and their early eucrite isochron to deduce a λ_{176Lu} value of $1.94\ 10^{-11}$ yr^{-1}, consistent with the determination of [45]. The error on this isochron, however, and the lack of a precisely known formation age for eucrites, limited the final precision of this result. More recently, [36] calibrated Lu–Hf ages obtained on igneous phosphates, gadolinite, and baddeleyite against the U–Pb ages of the same minerals and derived a precise λ_{176Lu} value of $1.865 \pm 0.015\ 10^{-11}\ yr^{-1}$. Finally, in contrast to the low mean value of the three most recent de-

terminations [36,46,47], a newly established statistically significant ^{176}Lu–^{176}Hf isochron on chondrites is consistent with a λ_{176Lu} value of $1.98 \pm 0.03\ 10^{-11}$ yr^{-1} (M. Bizzarro, unpublished data). In the following, the present Lu–Hf data on eucrites will be discussed using $\lambda_{176Lu} = 1.93\ 10^{-11}$ yr^{-1} [45], as this is the value that has been most commonly used in the past. Based on the outcome, we will evaluate whether this constant should be revised.

We have been unable to obtain a statistically significant ^{176}Lu–^{176}Hf eucrite isochron, whether leaving off cumulate eucrites and one outlier among the basaltic eucrites or not. Two options are possible. We can consider that the Lu–Hf system has been perturbed by impacts and that the small size of the samples analyzed combined with a large Lu/Hf fractionation among mineral phases (which contrasts with the Sm–Nd system) does not make it possible to define a whole-rock isochron. Alternatively, our estimate of the precision at which we measured the Lu/Hf ratios may have been too optimistic by a factor of two. Assuming, however, on a justification that still remains to be found, that a 1% error on this ratio instead of 0.5% (which is our current conservatively estimated error) provides statistically significant alignments, whether cumulate and basaltic eucrites are pooled or examined separately, the successful alignments still require that Palo Blanco Creek and Nagaria are excluded from the regressions. Surprisingly, the outliers are different for the Sm–Nd and the Lu–Hf systems. As was the case for the Sm–Nd system, the age indicated by the composite Lu–Hf isochron is dominated by the samples with high Lu/Hf ratios and Moama's leverage on the Lu–Hf isochron is 0.48. Excluding, therefore, the cumulate eucrites from the regression leaves an isochron of basaltic eucrites that is significantly older. The age deduced from this isochron is 100 Myr older than the age of the composite isochron and 140 Myr older than that of the Moama–Serra de Magé–Moore County alignment. It is noteworthy, that the ^{176}Lu–^{176}Hf age of these three cumulates is indistinguishable from the age indicated by the ^{147}Sm–^{144}Nd composite isochron, which we concluded is controlled by the cumulate eucrites.

Given the relatively large errors on the ^{176}Lu–^{176}Hf ages, the fact that the ages 'make sense' when applying the 'old' decay constant value for ^{176}Lu, and the coincidence of cumulate eucrite ages between the Lu–Hf and Sm–Nd systems, we do not consider that a revision of the ^{176}Lu decay constant with respect to the value of [45] is required (or justified) by the present data set. The most extreme constant suggested by [36] based on age comparisons with U–Pb in geological samples is the least satisfactory of the so far proposed constants, as an untenable age of ~4.75 Ga would result for the basaltic eucrites. However, since the statistical significance of our ^{176}Lu–^{176}Hf isochron is not unambiguously established, it is premature to discard this constant based on this argument. Furthermore, the age to be expected for eucrites is dependent on the details of early planetary evolution, which may not be sufficiently well known at present to be used to define a precise decay constant. However, the recent indication from chondritic meteorites (M. Bizzarro, unpublished data) of the possibility of a decay constant value slightly higher rather than lower with respect to that of [45] warrants caution against revision until more data become available. It also has to be understood why there seems to be a discrepancy between Lu decay constant calibrations based on extraterrestrial as compared to terrestrial materials, with the former indicating up to 6% faster decay than the latter.

4.3. *A combined Lu–Hf and Sm–Nd perspective on the differentiation of the eucrite parent body*

In most terrestrial igneous systems, the coherence between Hf and Nd isotopic data is extreme (e.g. [48,49]). In order to compare planetary objects with different evolutionary histories, we need to present their isotopic characteristics in a time-independent way. Since the Earth, Moon, and Mars all have post-formation histories, we chose to plot the eucrite data together with the data for these planets in the chondrite-normalized plot of source parent/daughter ratios used by [50] and [31] for lunar rocks and by [33] for shergottites. This plot (Fig. 3), which rests on a two-stage evolution model in which the intermediate event is

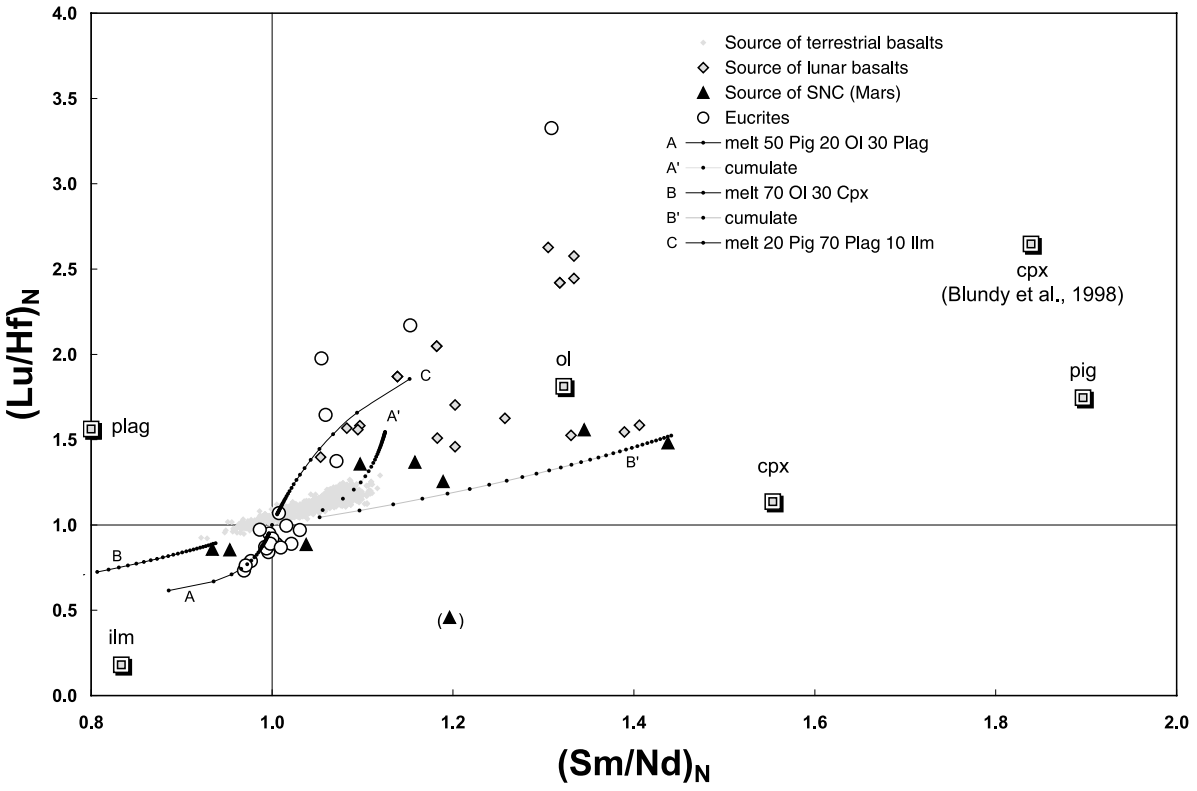

Fig. 3. Time-integrated $(Lu/Hf)_N$ vs. $(Sm/Nd)_N$ ratios of basalt sources on Earth, Moon, and Mars, compared with these ratios in eucrites. Source parent/daughter ratios were calculated for a source that differentiated at 4.56 Ga and evolved with radiogenic ingrowth at a constant parent/daughter ratio until the sample being measured was extracted from the mantle. As opposed to terrestrial, Martian, and lunar samples, eucrites have only a single-stage history. The appearance of the data in this diagram is essentially the same as in the conventional ε_{Hf}–ε_{Nd} diagram, with the exception that the data have been age corrected. Note that basaltic eucrites fall in the 'crustal' quadrant, whereas cumulate eucrites fall in the 'mantle' quadrant. The maximum slopes of the $(Lu/Hf)_N$ vs. $(Sm/Nd)_N$ correlations for the different planetary bodies increase in the order Earth, Mars, Moon, and Vesta, which we ascribe to the different thicknesses of the plagioclase stability field on the four planets. Lunar data are from [31,59] and SNC data from [33] and unpublished data of J. Blichert-Toft. The terrestrial mantle array is plotted from published and unpublished (J. Blichert-Toft) Hf and Nd isotope data for ~1800 mid-ocean ridge and ocean island basalts of worldwide distribution. The square symbols represent the Sm/Nd and Lu/Hf ratios in minerals in equilibrium with a chondritic melt [29,51–55]. Also shown is the composition of clinopyroxene in equilibrium with a melt of chondritic composition using the partition coefficients of Blundy et al. [56]. Two models of modal batch melting of a chondritic source using the same partition coefficients (melt and cumulate) illustrate the effect of variable plagioclase/(olivine+pyroxene) ratios in the residue. A model in which the source is an ilmenite-bearing gabbro is also shown (melt only). Contrary to crystallization models, which do not fractionate the Sm/Nd ratio, melting of late-stage ilmenite-bearing cumulates may account for the Sm/Nd and Lu/Hf correlation in cumulate eucrites and low-Ti lunar basalts.

the emplacement age, allows data for modern terrestrial basalts to be directly compared with other planetary data. As shown in Fig. 3, the correlation between $(Lu/Hf)_N$ and $(Sm/Nd)_N$ in eucrites is very strong ($\rho = 0.96$ for all eucrites, $\rho = 0.72$ for basaltic eucrites only) and would be even stronger had the ^{147}Sm–^{144}Nd system not been disturbed in Moama, the isotopically most extreme among the eucrites.

The slopes of the different planetary arrays in the $(Lu/Hf)_N$ vs. $(Sm/Nd)_N$ diagram steepen in the order of Earth, Mars, high-Ti lunar basalts, low-Ti lunar basalts and, finally, the eucrite parent body. Fig. 3 shows that for a given Sm/Nd ratio,

Lu/Hf fractionation was much stronger in eucrites and the source of low-Ti lunar basalts than in the terrestrial mantle. We also plotted individual minerals in equilibrium with a chondritic melt using measured (or interpolated) partition coefficients of [51] for olivine, [52] for pigeonite, [53] for clinopyroxene, [54] for plagioclase and [29,55] for ilmenite. These mineral values, which are essentially identical to those used by [31] for modeling lunar basalts, represent reasonably well the composition of cumulate minerals crystallizing from a magma ocean.

The present results on eucrites first of all demonstrate that the Lu/Hf ratio can be severely fractionated in melts without necessarily involving garnet in the residue. The key role of garnet has long been stressed as responsible for the Hf–Nd isotopic relationships in the sources of terrestrial [32,34], lunar [31], and Martian (SNC) [33] magmas. The fact that strong Lu/Hf fractionation combined with the usual Hf–Nd isotopic coherence is now also observed for the eucrite parent body, in which pressure conditions are inadequate to stabilize garnet, calls for new solutions to the so-called Hf paradox [34] when applied to the larger planets. Viable solutions with no garnet should bestow a more important role to residual clinopyroxene [56] and ilmenite (see below) during melting.

The ratios of incompatible elements such as Sm, Nd, Lu, and Hf hardly change during fractional crystallization until differentiation becomes extreme. The concentration ratio C_2/C_1 of two elements 1 and 2 changes with the fraction f crystallized as:

$$\frac{\Delta(C_2/C_1)}{(C_2/C_1)} \approx (D_1 - D_2)\frac{\Delta f}{1-f}$$

where D stands for bulk solid–liquid partition coefficients. The large changes in Lu/Hf ratios (several 10%) and strong correlation between $(Lu/Hf)_N$ vs. $(Sm/Nd)_N$ therefore require that eucrites are partial melts and not simple residual liquids. A similar conclusion was reached for the source of low-Ti lunar basalts by [31]. We have calculated the Lu/Hf and Sm/Nd ratios in a series of melts as well as the corresponding cumulates equilibrated with these melts, using the equation of so-called modal batch equilibrium melting for a number of residual mineral assemblages (A, B, C). Although this equation is unlikely to represent the melting conditions adequately (e.g. [31,57]), it still illustrates melting trends in the $(Lu/Hf)_N$ vs. $(Sm/Nd)_N$ diagram reasonably well.

One interpretation of the main group of basaltic eucrites is that they represent large-degree melts of a chondritic planetary body [8] leaving an olivine ± clinopyroxene ± pigeonite+plagioclase (i.e., a gabbroic) residue. In this respect, the eucrite array differs from the terrestrial mantle array whose shallower slope points toward an essentially plagioclase-free (ultramafic) assemblage (Fig. 3). The degree of melting of such a parent melt of basaltic eucrites must have been large enough (i.e., $>10\%$) that Sm/Nd and Lu/Hf fractionation between the source and the melt remained relatively small. The large negative Eu anomalies observed in some basaltic eucrites [57,58] confirm the presence of residual plagioclase in their source. The Fe-poor character of both Serra de Magé and Moore County makes them unsuitable as cumulates or residues in equilibrium with eucritic melts [8]. An alternative interpretation is that basaltic eucrites may have been produced as small-degree melts of the pigeonite+plagioclase ± olivine cumulates thought to form upon cooling of an asteroidal (Vesta) magma ocean [9]. A source intermediate in composition to diogenites and Serra de Magé or, to a lesser extent Moore County, would probably be acceptable.

The amplitude of $(Lu/Hf)_N$ and $(Sm/Nd)_N$ variations in cumulate eucrites and the steep slope of their correlation cannot be the result of crystal fractionation alone. In this case, the trend should have been near-vertical with negligible Sm/Nd variation. The Lu/Hf ratios of the cumulate eucrites exceed the ratio for any combination of rock-forming minerals that would evolve from melts with nearly chondritic trace element distributions. Not even with the rather extreme clinopyroxene/melt partition coefficients of [56] can this conclusion be reverted (Fig. 3). The formation of cumulate eucrites therefore needs the intervention of an additional process that removes

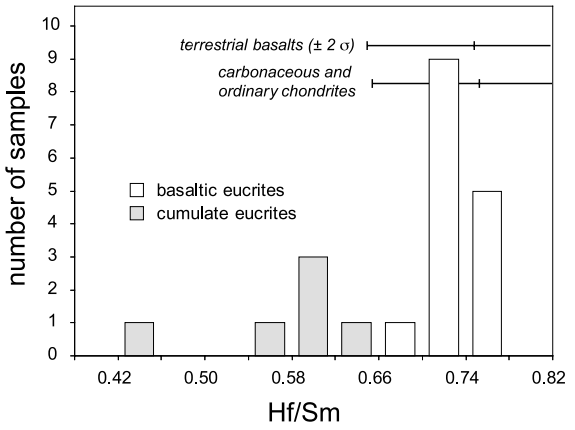

Fig. 4. The Hf/Sm ratio of basaltic and cumulate eucrites compared with the same ratio in terrestrial basalts (2σ range, our own unpublished compilation) and meteorites [65]. This ratio remains essentially unfractionated by magmatic processes until ilmenite saturation is reached.

Hf from the melt and enhances Lu/Hf fractionation. The only mineral known from eucrites that incorporates enough Hf to account for the large observed Lu/Hf fractionation is ilmenite (e.g. [55]). Moama, and to a lesser extent Serra de Magé and Moore County, share the high Lu/Hf characteristic with the source of low-Ti lunar basalts [31,59]. The presence of residual ilmenite when the parent melt of cumulates formed is particularly visible from the low Hf/Sm ratios of cumulate eucrites (Fig. 4). In basaltic eucrites, as in most terrestrial and lunar basalts, this ratio is extremely constant and chondritic (Hf/Sm $\sim 0.75 \pm 0.12$), reflecting that both Hf and Sm are incompatible to the same extent (e.g. [60]). In contrast, this ratio in cumulate eucrites falls in the range 0.4–0.6, which is significantly lower than the chondritic value. It is quite remarkable that such low ratios are also found in nakhlites and chassignites [33], which are ultramafic cumulates of what must have been differentiated Martian basalts. As for lunar basalts [61], ilmenite saturation is only achieved after extensive fractionation, probably on the order of 90%. The correlation between Lu/Hf and Sm/Nd therefore suggests a partial melt with ilmenite in the residue controlled the distribution of these elements in the cumulate eucrites. The low Ti contents and low Fe/Mg ratios of cumulate eucrites [8,57] are consistent with the presence of refractory ilmenite during fusion. Whether the source of this partial melt is analogous to frozen-in eucrites or mafic cumulates cannot be resolved by the present data. Impregnation of a gabbroic crust by such partial melts currently is our best model for the origin of cumulate eucrites.

5. Conclusions

Whole-rock eucrites form a statistically significant Sm–Nd isochron, whereas the corresponding Lu–Hf data form such an alignment only if the analytical error on the Lu/Hf ratios is doubled with respect to our current estimate. The two systems otherwise convey consistent chronometric information. The present study suggests that cumulate eucrites are about 100 Myr younger than basaltic eucrites and that basaltic eucrites are about the age of the Solar System. The initial $^{176}Hf/^{177}Hf$ of the Solar System is 0.27966 ± 0.00002. There is no indication from the present Lu–Hf isotope data that the decay constant of ^{176}Lu of $1.93\ 10^{-11}\ yr^{-1}$ [45] is in need of significant revision.

The broad range of variation and strong correlation of Lu/Hf and Sm/Nd ratios in eucrites suggest they are partial melts and not residual magmas. The steep correlation between these two trace element ratios is explained by the enhancement of plagioclase saturation in the low-gravity field of the eucrite parent body. Strong Lu/Hf and Sm/Hf fractionation is observed that clearly reflects the presence of residual ilmenite during melting and questions the presence of residual garnet in the mantle sources of magmas formed on larger planets.

Acknowledgements

We are particularly grateful to the meteorite curators of the Muséum National d'Histoire Naturelle de Paris, Michèle Denise, Geologisk Museum of Copenhagen, Asger Ken Pedersen, The Natural History Museum of London, Monica Grady, Museum Victoria in Melbourne, Bill

Birch, the National Museum of Natural History of the Smithsonian Institution in Washington DC, Glenn MacPherson, and the Naturhistorisches Museum in Vienna, Gero Kurat, for having showed us confidence and generously provided all the meteorite samples that formed the basis for this study. Insightful reviews by Richard Carlson, Günter Lugmair, and Erik Scherer helped us revise our conclusions substantially. Ken Ludwig suggested the solution to our MSWD anguish. Martin Bizzarro and Henning Haack kindly shared detailed advance information on their newly established chondrite isochron. We further thank Chris MacIsaac for providing La Jolla Nd standard and Sm and Nd Ames metal solutions for spike calibration purposes. Finally, we acknowledge the French Institut National des Sciences de l'Univers and the Programme National de Planétologie for financial support. *[BW]*

Appendix A. Statistical data treatment

The Lu–Hf and Sm–Nd isotope data were processed using an in-house isochron software derived from the original program written by [62] and described in detail by [41]. This software, available from the ftp site ftp.ens-lyon.fr/pub/users/GEOL/albarede, was written in MatLab for high-precision arithmetics and extensively tested against Monte-Carlo error propagation experiments. It replicates results obtained using Microsoft Excel-based software written by [63]. All errors reported are straight propagated errors. In the geochemical community, it is common practice to report the vertical deviation of all data points from the isochron (the so-called δY plot) as a way of assessing which points fall significantly off the alignment. This practice, however, ignores the fact that regression acts in both the X and Y directions and that the adjusted point can be at any angle to the original measurement. Whether a point is potentially an outlier can be better assessed from the reduced residual χ_i, where:

$$\chi_i^2 = \frac{(y_i - ax_i - b)^2}{\sigma_{y,i}^2 + a^2\sigma_{x,i}^2}$$

with x_i and y_i standing for the abscissa and ordinate of the i-th point, a and b for the slope and intercept, respectively, and σ for the appropriate standard deviations. There is no ambiguity involved with using a chi notation since the sum of the squared χ_is over the n points is a chi-squared random variable with $n-2$ degrees of freedom and an expected value of $n-2$. A χ_i^2 value significantly larger than one therefore signals a point with dubious fit.

In the least-square isochron theory, two parameters, the slope and the intercept, are determined from the alignment of a number of data points. The importance (or leverage, see [41]) of a datum is the fraction of one parameter that it contributes to determine. For a straight line, the number of independent parameters is two and leverage numbers sum to two. During the regression, the data are associated through an appropriate projection with their so-called adjusted values. The projector is a square diagonal-dominant symmetric matrix, which is described in a number of books (e.g. [41,64]). The diagonal entries sum to the number of independent parameters, here two. If the i-th diagonal entry is equal to one, this simply expresses the fact that the measured and the adjusted values are identical and that the regression line goes through this particular data point. This is the case for a two-point isochron, for which each datum contributes the equivalent of one full parameter. A mean leverage value of $n/2$ would signal a robust isochron for which the slope and intercept do not depend too much on a few particular points.

References

[1] R.N. Clayton, T.K. Mayeda, Oxygen isotope studies of achondrites, Geochim. Cosmochim. Acta 60 (1996) 1999–2017.
[2] U. Wiechert, A.N. Halliday, H. Palme, D. RumbleIII, Oxygen isotopic heterogeneity among eucrites, Geochim. Cosmochim. Acta 66 (2002) A834.
[3] O. Eugster, T. Michel, Common asteroid break-up events of eucrites, diogenites, and howardites and cosmic-ray production rates for noble gases in achondrites, Geochim. Cosmochim. Acta 59 (1995) 177–199.
[4] K.C. Welten, L. Lindner, K. vanderBorg, T. Loeken, P. Scherer, L. Schultz, Cosmic-ray exposure ages of dio-

genites and the recent collisional history of the howardite, eucrite and diogenite parent body/bodies, Meteorit. Planet. Sci. 32 (1997) 891–902.
[5] G.J. Consolmagno, M.J. Drake, Composition and evolution of the eucrite parent body: evidence from rare earth elements, Geochim. Cosmochim. Acta 41 (1977) 1271–1282.
[6] T.B. McCord, J.B. Adams, T.V. Johnson, Asteroid Vesta: spectral reflectivity and compositional implications, Science 168 (1970) 1445–1447.
[7] R.P. Binzel, S. Xu, Chips off of asteroid 4 Vesta: evidence for the parent body of basaltic achondrite meteorites, Science 260 (1993) 186–191.
[8] E. Stolper, Experimental petrology of eucrite meteorites, Geochim. Cosmochim. Acta 41 (1977) 587–611.
[9] K. Righter, M.J. Drake, A magma ocean on Vesta: core formation and petrogenesis of eucrites and diogenites, Meteorit. Planet. Sci. 32 (1997) 929–944.
[10] B.L. Jolliff, J.J. Gillis, L.A. Haskin, R.L. Korotev, M.A. Wieczorek, Major lunar crustal terranes: surface expressions and crust-mantle origins, J. Geophys. Res. 105 (2000) 4197–4216.
[11] A.E. Ringwood, S.E. Kesson, A dynamic model for mare basalt petrogenesis, Proc. Lunar Sci. Conf. 7 (1976) 1697–1722.
[12] S.R. Taylor, P. Jakes, The geochemical evolution of the Moon, Proc. Lunar Sci. Conf. 5 (1974) 1287–1305.
[13] S.R. Taylor, The origin of the Moon: geochemical considerations, in: W.K. Hartmann, R.J. Phillips, G.J. Taylor (Eds.), Origin of the Moon, Lunar and Planetary Institute, Houston, TX, 1986, pp. 125–143.
[14] H.Y. McSween Jr., Achondrites and igneous processes on asteroids, Annu. Rev. Earth Planet. Sci. 17 (1989) 119–140.
[15] D.W. Mittlefehldt, T.J. McCoy, C.A. Goodrich, A. Kracher, Non-chondritic meteorites from asteroidal bodies, in: J.J. Papike (Ed.), Planetary Materials, Reviews in Mineralogy 36, Mineralogical Society of America, Washington, DC, 1998, pp. 4: 1–195.
[16] G.W. Lugmair, Sm–Nd ages: a new dating method, Meteoritics 9 (1974) 369.
[17] G.W. Lugmair, N.B. Scheinin, Sm–Nd systematics of the Stannern meteorite, Meteoritics 10 (1975) 447–448.
[18] L.E. Nyquist, H. Takeda, B.M. Bansal, C.-Y. Shih, H. Wiesmann, J.L. Wooden, Rb–Sr and Sm–Nd internal isochron ages of a subophitic basalt clast and a matrix sample from the Y75011 eucrite, J. Geophys. Res. 91 (1986) 8137–8150.
[19] M. Wadhwa, G.W. Lugmair, Age of the eucrite 'Caldera' from convergence of long-lived and short-lived chronometers, Geochim. Cosmochim. Acta 60 (1996) 4889–4893.
[20] F. Tera, R.W. Carlson, N.Z. Boctor, Radiometric ages of basaltic achondrites and their relation to the early history of the Solar System, Geochim. Cosmochim. Acta 61 (1997) 1713–1731.
[21] G.W. Lugmair, A. Shukolyukov, Early solar system timescales according to ^{53}Mn–^{53}Cr systematics, Geochim. Cosmochim. Acta 62 (1998) 2863–2886.
[22] L.E. Nyquist, Y. Reese, H. Wiesmann, C.-Y. Shih, H. Takeda, Live ^{53}Mn and ^{26}Al in a unique cumulate eucrite with very calcic feldspar (An ~98), Meteorit. Planet. Sci. Suppl. 36 (2001) A151–A152.
[23] A. Shukolyukov, G.W. Lugmair, ^{60}Fe in eucrites, Earth Planet. Sci. Lett. 119 (1993) 159–166.
[24] G. Srinivasan, D.A. Papanastassiou, G.J. Wasserburg, N. Bhandari, J.N. Goswami, Re-examination of ^{26}Al–^{26}Mg systematics in the Piplia Kalan eucrite. Lunar Planet. Sci. XXXI (2000) A1795.
[25] G.W. Lugmair, N.B. Scheinin, R.W. Carlson, Sm–Nd systematics of the Serra de Magé eucrite, Meteoritics 12 (1977) 300–301.
[26] J. Hamet, N. Nakamura, D.M. Unruh, M. Tatsumoto, Origin and history of the adcumulate eucrite, Moama as inferred from REE abundances, Sm–Nd and U–Pb systematics, Proc. Lunar Planet. Sci. Conf. 9 (1978) 1115–1136.
[27] P.J. Patchett, M. Tatsumoto, Lu–Hf total-rock isochron for the eucrite meteorites, Nature 288 (1980) 571–574.
[28] M. Tatsumoto, D.M. Unruh, P.J. Patchett, U–Pb and Lu–Hf systematics of Antarctic meteorites, Proc. 6th Symp. Antarctic meteorites. Natl. Inst. Polar Res., Tokyo, 1981, pp. 237–249.
[29] G. McKay, J. Wagstaff, S.-R. Yang, Zirconium, hafnium, and rare earth element partition coefficients for ilmenite and other minerals in high-Ti lunar mare basalts: an experimental study, J. Geophys. Res. 91 (1986) D229–D237.
[30] Y. Nakamura, H. Fujimaki, N. Nakamura, M. Tatsumoto, G.A. McKay, J. Wagstaff, Hf, Zr, and REE partition coefficients between ilmenite and liquid: implications for lunar petrogenesis, J. Geophys. Res. 91 (1986) D239–D250.
[31] B.L. Beard, L.A. Taylor, E.E. Scherer, C.M. Johnson, G.A. Snyder, The source region and melting mineralogy of high-titanium and low-titanium lunar basalts deduced from Lu–Hf isotope data, Geochim. Cosmochim. Acta 62 (1998) 525–544.
[32] J. Blichert-Toft, F. Albarède, The Lu–Hf isotope geochemistry of chondrites and the evolution of the mantle-crust system, Earth Planet. Sci. Lett. 148 (1997) 243–258.
[33] J. Blichert-Toft, J.D. Gleason, P. Télouk, F. Albarède, The Lu–Hf isotope geochemistry of shergottites and the evolution of the Martian mantle-crust system, Earth Planet. Sci. Lett. 173 (1999) 25–39.
[34] V.J.M. Salters, S.R. Hart, The hafnium paradox and the role of garnet in the source of mid-ocean-ridge basalts, Nature 342 (1989) 420–422.
[35] F. Begemann, K.R. Ludwig, G.W. Lugmair, K. Min, L.E. Nyquist, P.J. Patchett, P.R. Renne, C.-Y. Shih, I.M. Villa, R.J. Walker, Call for an improved set of decay constants for geochronological use, Geochim. Cosmochim. Acta 65 (2001) 111–121.
[36] E. Scherer, C. Münker, K. Mezger, Calibration of the lutetium–hafnium clock, Science 293 (2001) 683–687.

[37] J. Blichert-Toft, C. Chauvel, F. Albarède, Separation of Hf and Lu for high-precision isotope analysis of rock samples by magnetic sector-multiple collector ICP-MS, Contrib. Mineral. Petrol. 127 (1997) 248–260.
[38] J. Blichert-Toft, On the Lu–Hf isotope geochemistry of silicate rocks, Geostand. Newsl. 25 (2001) 41–56.
[39] B. Luais, P. Télouk, F. Albarède, Precise and accurate neodymium isotopic measurements by plasma-source mass spectrometry, Geochim. Cosmochim. Acta 61 (1997) 4847–4854.
[40] C.N. Maréchal, P. Télouk, F. Albarède, Precise analysis of copper and zinc isotopic compositions by plasma-source mass spectrometry, Chem. Geol. 156 (1999) 251–273.
[41] F. Albarède, Introduction to Geochemical Modeling, Cambridge University Press, Cambridge, 1995, 543 pp.
[42] S.B. Jacobsen, G.J. Wasserburg, Sm–Nd isotopic evolution of chondrites, Earth Planet. Sci. Lett. 50 (1980) 139–155.
[43] J. Kunz, M. Falter, E.K. Jessberger, Shocked meteorites: argon-40–argon-39 evidence for multiple impacts, Meteorit. Planet. Sci. 32 (1997) 647–670.
[44] D.D. Bogard, Impact ages of meteorites: a synthesis, Meteoritics 30 (1995) 244–268.
[45] A.P. Sguigna, A.J. Larabee, J.C. Waddington, The half-life of ^{176}Lu by a γ-γ coincidence measurement, Can. J. Phys. 60 (1982) 361–364.
[46] J. Dalmasso, G. Barci-Funel, G.J. Ardisson, Reinvestigation of the decay of the long-lived odd-odd ^{176}Lu nucleus, Appl. Radiat. Isot. 43 (1992) 69–76.
[47] Y. Nir-El, N. Lavi, Measurement of the half-life of ^{176}Lu, Appl. Radiat. Isot. 49 (1998) 1653–1655.
[48] P.J. Patchett, M. Tatsumoto, Hafnium isotope variations in oceanic basalts, Geophys. Res. Lett. 7 (1980) 1077–1080.
[49] J.D. Vervoort, J. Blichert-Toft, Evolution of the depleted mantle: Hf isotope evidence from juvenile rocks through time, Geochim. Cosmochim. Acta 63 (1999) 533–556.
[50] L.E. Nyquist, C.-Y. Shih, The isotopic record of lunar volcanism, Geochim. Cosmochim. Acta 56 (1992) 2213–2234.
[51] A.K. Kennedy, G.E. Lofgren, G.J. Wasserburg, An experimental study of trace element partitioning between olivine, orthopyroxene and melt in chondrules: equilibrium values and kinetic effects, Earth Planet. Sci. Lett. 115 (1993) 177–195.
[52] G.A. McKay, J. Wagstaff, L. Le, REE distribution coefficients for pigeonite: constraints on the origin of the mare basalt europium anomaly, III, in: Mare Volcanism and Basalt Petrogenesis Workshop, LPI Tech. Rept. 91-03, 1991, pp. 27–28.
[53] S.R. Hart, T. Dunn, Experimental cpx/melt partitioning of 24 trace elements, Contrib. Mineral. Petrol. 113 (1993) 1–8.
[54] W.C. Phinney, D.A. Morrison, Partition coefficients for calcic plagioclase: implications for Archean anorthosites, Geochim. Cosmochim. Acta 54 (1990) 1639–1654.
[55] H. Fujimaki, M. Tatsumoto, K.-i. Aoki, Partition coefficients of Hf, Zr, and REE between phenocrysts and groundmasses, J. Geophys. Res. 89 (1984) B662–B672.
[56] J.D. Blundy, J.A.C. Robinson, B.J. Wood, Heavy REE are compatible in clinopyroxene on the spinel lherzolite solidus, Earth Planet. Sci. Lett. 160 (1998) 493–504.
[57] J.A. Barrat, J. Blichert-Toft, P. Gillet, F. Keller, The differentiation of eucrites: the role of in situ crystallization, Meteorit. Planet. Sci. 35 (2000) 1087–1100.
[58] C.C. Schnetzler, J.A. Philpotts, Alkali, alkaline earth and rare earth element concentrations in some Apollo 12 soils, rocks and separated phases, Proc. Lunar Sci. Conf. 2 (1971) 1101–1122.
[59] D.M. Unruh, P. Stille, P.J. Patchett, M. Tatsumoto, Lu–Hf and Sm–Nd evolution in lunar mare basalts, J. Geophys. Res. 89 (1984) B459–B477.
[60] A.W. Hofmann, Chemical differentiation of the Earth: the relationship between mantle, continental crust, and oceanic crust, Earth Planet. Sci. Lett. 90 (1988) 297–314.
[61] L.T. Elkins Tanton, J.A. VanOrman, B.H. Hager, T.L. Grove, Re-examination of the lunar magma ocean cumulate overturn hypothesis: melting or mixing is required, Earth Planet. Sci. Lett. 196 (2002) 239–249.
[62] J.-F. Minster, P. Ricart, C.J. Allègre, ^{87}Rb–^{87}Sr geochronology of enstatite meteorites, Earth Planet. Sci. Lett. 42 (1979) 333–347.
[63] K.R. Ludwig, ISOPLOT: A plotting and regression program for radiogenic isotope data. USGS Open File Report, 1991, pp. 91–445.
[64] A. Sen, M. Srivastava, Regression Analysis. Theory, Methods, and Applications, Springer-Verlag, New York, 1990.
[65] H.E. Newsom, Composition of the solar system, planets, meteorites, and major terrestrial reservoirs, in: T.J. Ahrens (Ed.), Global Earth Physics. A Handbook of Physical Constants, AGU reference shelf 1, AGU, Washington, DC, 1995, pp. 159–189.